

Modelling by FEM the Effect of the Morphological Modifications of the Superalloys γ/γ'

M. Massaoudi and L. Durand

*CEMES/CNRS -- 29 rue Jeanne Marvig / BP 94347 – 31055 Toulouse Cedex 04
durand@cemes.fr*

ABSTRACT

The turbine blades of the turbojet are hollow parts and their cooling is done by circulation of air; their operating temperature is estimated between 750°C and 1100°C : the behaviour of the superalloys is then rather complex; the microstructure initially cuboidal evolves in a structure (coarsened) in alternate plates of γ and γ' phases so called “in rafts”.

The macroscopic model limitations, noted in former studies, lead us in this article to take into account the effect of the hydrostatic pressure for cuboid microstructures. From there, various modellings and calculations on the coarsened structures are carried out to describe in a correct way their morphological evolutions.

It is noted that the introduction of the effect of the hydrostatic pressure allows better modelling of the effects of the morphological modifications observed in the superalloys. The simulated curves show a good agreement between the finite elements calculations and experimental results. The stress and strain state approaches the real behaviour of the superalloys in service.

Keywords: Superalloys, rafts, viscoplasticity, hydrostatic pressure, finite elements method, macroscopic model.

1. INTRODUCTION

At high temperatures, the local mechanisms of dislocations, in the superalloys, lead to strong modifications of the structure, in particular that of the precipitates. Above the temperature of approximately 950°C, when a superalloy is creeping in a uniaxial direction $\langle 001 \rangle$, its microstructure evolves into alternate plates of phases γ and γ' ; this evolution makes their behaviour more complex; it consists of directionally coarsened precipitates which appear from the first hours of service in the hot parts of the turbine blades subjected to the centrifugal force. This microstructural evolution is known as “setting in rafts”.

Two parameters have attracted the interest of several authors in the study of coarsening: the influence of volume fraction, the misfit role. Thus studies of coarsening with or without external load with the influence of the sign of the applied pressure, the size of the channels, whose measurements allow the quantification of the evolution of the precipitate morphologies, of the dislocations in γ/γ' interfaces of the coarsened microstructures, etc..., have been carried out.

Coarsening without external pressure has led to many studies where the volume fraction and the misfit represent the most important parameters associated with the elastic characteristics of both phases. Cornet *et al.* concluded that in the field of strong volume fractions, the transformation of the cuboids into plates is strongly facilitated /1/. The volume fraction, particularly when it is high, plays a determining part in the coarsening process /2/. However, at the temperatures where coarsening is established, the volume fraction seems to evolve little, which generates a problem in the study of this parameter.

For an alloy, evolving without applied pressure, the misfit generates alone fields of elastic strain. Muralidharan *et al.* propose that for small values of misfit, the initial increase in the coarsening rate is primarily due to an increase in the elastic energy of interaction /3/.

However, in the presence of an applied pressure, emphasizing the influence of the misfit is complicated insofar as the contributions to elastic energy are added. Experimental observations have shown that the misfit stress just like the applied pressure are important for the evolution of the morphology of the coarsened γ' precipitates /4/.

The applied stress's sign influence on a structure in rafts has been the subject of many studies. Indeed, the sign of this stress is determining for the knowledge of the rafts shape; under a tensile stress, the rafts are perpendicular to this stress's axis, whereas under a compression, they are parallel to it, i.e. the term of directional coarsening (Figure 1). By convention, in the whole of the literature "morphology P" indicates that the rafts plane is parallel to the request axis, and "morphology N" characterizes those whose plane is normal to this same axis (Figure 2). The electron microscopy observations of the two phases show that the matrix channels are thicker in the case of cuboid morphology /5/; but few relevant parameters are apt to account for the forms met, which makes the analysis of coarsening morphologies rather difficult.

The contribution of the elastic interactions between particles increases in the presence of an applied stress; this shows the importance of the size and the distribution of the matrix corridors.

Moreover, several authors showed much interest in the measurement of the size of the channels in the hope of quantifying the evolutions of the morphology of the precipitates /6, 7, 8/. Other authors are leaning towards the realization of microstructures coarsened by fatigue /9/, or by creep stresses /10, 11 /. The first way highlights the importance of the kinetics of diffusion, whereas the second shows that temperatures lower than 1000°C are without interest because of too weak coarsening kinetics. In general, the microstructures obtained by these two methods are more or less similar.

We noted the difficulties experienced by the various models that describe coarsening present in the literature /12/. Several authors were directed towards the finite elements method in order to evaluate the parameters controlling the microstructural evolution for a better understanding of the coalescence and thus

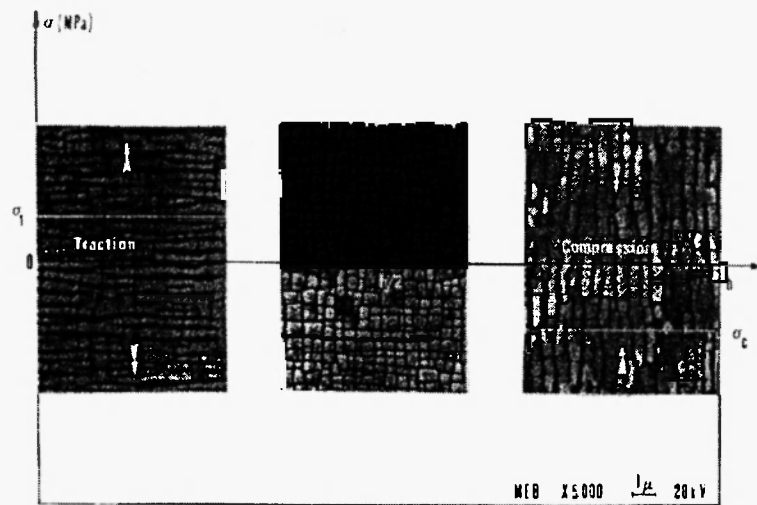


Fig. 1: Illustration of various morphologies observed; the figure on the left corresponds to a morphology of type N and the figure on the right corresponds to a morphology of type P. /11/.

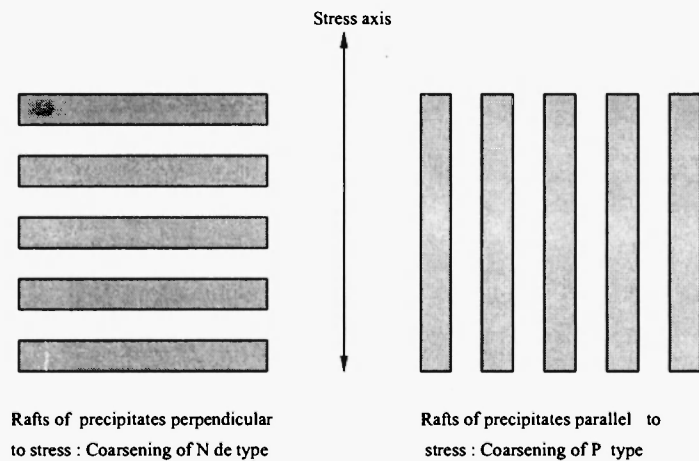


Fig. 2: Directional coarsening : morphologies obtained on single crystals of orientation [001].

study the various possible contributions. The finite element calculations carried out /5, 13, 14/ confirm the importance of some parameters related to the precipitate morphology in the finite elements model, such as the volume fraction and the size of the precipitate in the three directions, in addition to the matrix corridor size. These parameters allow the improvement of the results of finite element calculations.

From the critical analysis of these finite elements approaches, one notes:

- the importance of the dimensions, and the distribution of the coarsened precipitates and that of distribution of the matrix corridor,
- the important role of the misfit since it introduces local stresses into the coarsened microstructures and thus induces elastic fields that dislocations come to disturb,
- the role of the applied pressure which modifies these local stresses and introduces dislocations,
- the importance of a meshed structure corresponding to the microstructural observations,
- the necessity of a three-dimensional approach,
- the overestimation of the calculated stresses, making difficult real conclusions,
- the necessity of the correct estimate of the local state of stresses, and especially of the stress fields around the precipitates.

The finite elements calculations presented here are carried out in the first section on cuboidal microstructures in order to evaluate the influence of the hydrostatic pressure on the superalloys' behaviour, by modifying the constitutive equations of the matrix behaviour law; the results of these calculations are presented and discussed. Then, we study the effect of the morphological modifications of the superalloys' microstructures. Finite element calculations are carried out at the temperature of 950°C for coarsened morphologies of type "P", "N" and "plate". The simulation results are compared with the experimental data of the literature.

2. HYDROSTATIC PRESSURE INFLUENCE

The macroscopic model's limitations, noted previously in representing simultaneously $\langle 001 \rangle$ traction and pure shearing, lead to a modification of the equations of matrix behaviour law. However, the modifications of the microstructure geometry of the superalloy seem not to bring any solution /15/.

Moreover the derived models are implemented supposing that the material is homogeneous, which is contrary to reality. They do not account for the influence of the microstructural evolution of the superalloys, observed at high temperature: by "the Poisson effect"; the plastic strain tends to concentrate round the intersection of the fine matrix corridors (very narrow zones).

A solution suggested by D. Nouailhas /16/ and J L Chaboche /15/, consists in taking into account hydrostatic pressure in this model. We propose, in this section, to reconsider and expand this idea.

Although at high temperature, the experimental literature does not note the shearing of the precipitates, we propose to determine the distribution of the hydrostatic pressure in the material, by authorizing the plasticization of the precipitate. In this part, we do not take into account the internal stresses due to the misfit.

2.1. Matrix behaviour law

In order to redistribute the important hydrostatic pressure, we explore the idea suggested by Nouailhas *et al.* / 16 / and Chaboche *et al.* / 15 / which consists in taking into account the effect of the hydrostatic pressure in the behaviour law of the matrix.

For that, the behaviour law of the matrix is amended so that the effect of the hydrostatic pressure is introduced into the viscoplasticity criterion, leading thus, via the classical hypothesis of normality, to a compressible plastic matrix.

Table 1 summarizes the equations of the model. They are expressed in the crystallographic reference.

We introduce into the expression of the threshold function, the tensor of stress σ without any modification, instead of σ' deviative tensor; $\sigma - \sigma'$ is the hydrostatic pressure tensor. The introduction of the

Table 1
Equations of macroscopic model with the hydrostatic pression effect.

$\epsilon_{tot} = \epsilon^e + \epsilon^v$	(1)
$\sigma_{ij} = C_{ijkl} : \epsilon_{kl}^e$	(2)
$\Omega = \frac{K}{n+1} \langle \frac{f}{K} \rangle^{n+1}$	(3)
$f = \left\{ \left(\left[\frac{3}{2} (a'_1 I_1 + 2a'_2 I_2 + 2a'_4 I_4) \right]^2 + 3a'_8 I_8 \right)^3 - (a'_6 I_6)^4 \right\}^{\frac{1}{12}} - k$	(4)
$\begin{cases} I_1 = (\sigma_{11} - X_{11})^2 + (\sigma_{22} - X_{22})^2 + (\sigma_{33} - X_{33})^2 \\ I_2 = (\sigma_{11} - X_{11})(\sigma_{22} - X_{22}) + (\sigma_{22} - X_{22})(\sigma_{33} - X_{33}) + (\sigma_{11} - X_{11})(\sigma_{33} - X_{33}) \\ I_4 = (\sigma_{23} - X_{23})^2 + (\sigma_{31} - X_{31})^2 + (\sigma_{12} - X_{12})^2 \\ I_6 = (\sigma_{23} - X_{23})(\sigma_{31} - X_{31})(\sigma_{12} - X_{12}) \\ I_8 = (\sigma_{23} - X_{23})^3 + (\sigma_{31} - X_{31})^3 + (\sigma_{12} - X_{12})^3 \end{cases}$	(5)
$\dot{\epsilon}_{ij}^p = \frac{\partial \Omega}{\partial \sigma_{ij}} = \dot{p} \frac{\partial f}{\partial \sigma_{ij}}$	(6)
$\dot{p} = \langle \frac{f}{K} \rangle^n$	(7)
$\begin{cases} X_{ij} = X_{ij}^1 + X_{ij}^2 \\ X_{ij}^1 = \frac{2}{3} C^1 A_{ijkl}^1 \alpha_{kl}^1 \\ X_{ij}^2 = \frac{2}{3} C^2 A_{ijkl}^2 \epsilon_{kl}^p \end{cases}$	(8)
$\dot{\alpha}_{ij}^1 = \dot{\epsilon}_{ij}^p - D^1 B_{ijkl}^1 \alpha_{kl}^1 \dot{p}$	(9)

invariant I_1 , into the viscoplasticity criterion allows then the implementation of the hydrostatic pressure effect.

The macroscopic criterion is established in such a way that material symmetries are respected, the initial anisotropy being well described, the σ_{ij} represent the stresses tensor components, and the coefficients (a_i) are constants. The viscoplastic flow law results from equation 3 by complying with the rule of normality. p -describes the cumulated plastic (viscoplastic) strain evolution. Threshold surface relocates according to evolution laws of the kinematic variable α (tensorial). Two tensors of order four allow the linear and nonlinear kinematic hardening variables (respectively X^2 and X^1) to describe the anisotropy induced by the plastic strain.

The components of the tensors A_{ijkl} and B_{ijkl} , with the bottom indices according to the Voigt notation and $k = 1, 2$, in the cubic symmetry case, are such as :

$$\begin{aligned} A^k_{11} &= A^k_{22} = A^k_{33} = 1 \\ A^k_{44} &= A^k_{55} = A^k_{66} = A^1 \\ B^1_{11} - B^1_{22} &= B^1_{33} = 1 \\ B^1_{44} - B^1_{55} - B^1_{66} &= B^1 \end{aligned}$$

the other components A^k_{ij} and B^1_{ij} where $i \neq j$ are null.

2.2 Preliminary results

The following calculations are developed by imposing a uniform displacement until a strain of 2%, along the [001] axis has been produced.

Figure 3 shows the distribution of the hydrostatic pressure in the matrix. The values obtained are coherent with those obtained by D. Nouailhas /16/. Figure 4 represents the distribution of plastic strain ϵ^p_{33} in the

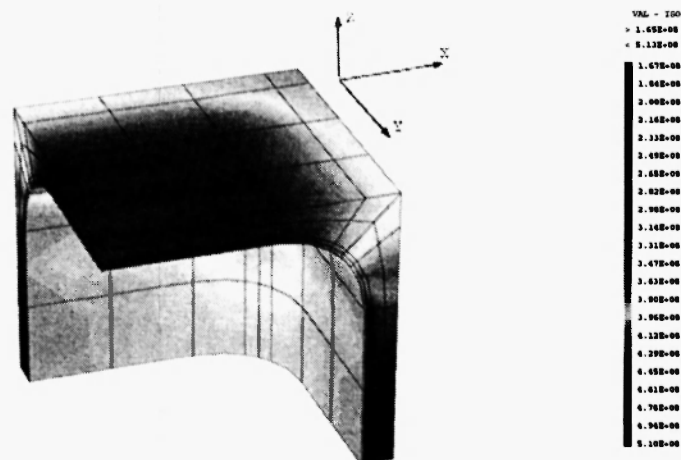


Fig. 3: Hydrostatic pressure distribution (in Pa) in the matrix.

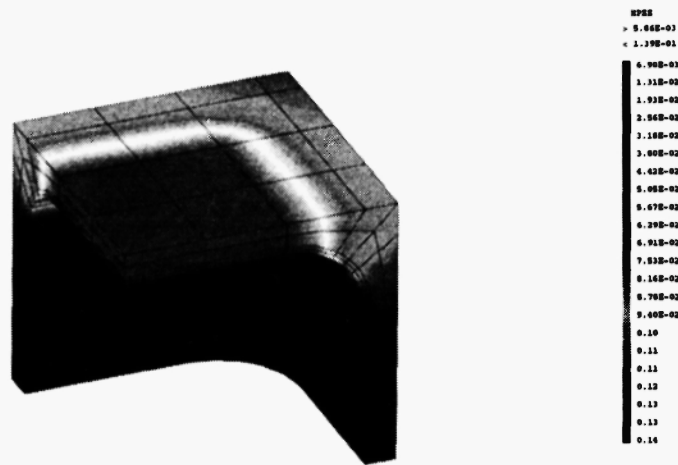


Fig. 4: ϵ^P_{33} strains distribution in the γ matrixe.

matrix channels. We note that in the channel perpendicular to the action axis ([001]), the strain is uniform; this result is also in agreement with that of Nouailhas /16/. Through these calculations, we find the same results as the authors quoted above; at this stage, for a strain lower than 2 %, the modification of the matrix flow has only little influence.

In the following stage we propose to plasticize the precipitate. The results of calculations are shown in Figures 5 and 6. The hydrostatic pressure distribution in the matrix is less intense compared with the preceding case. These figures show then that the assumption of an effect of hydrostatic pressure according to the formulation given in 4 allows finally a better redistribution of the hydrostatic stresses, and the plastic strains are in the narrowest zones. It seems that the experimental results go in this direction, it would be interesting to confirm or invalidate this point in electron microscopy.

However, as the volume fraction of the precipitates becomes the higher, the matrix is more confined in a very small distance; this generates a major difficulty of this type of calculation insofar as the precipitate becomes the only pilot of the dislocations movement. Up to now, however, there has been no model that allows the simulation of the interaction between the precipitates and dislocations. This shows that for these materials, the physical phenomena play on a scale so small that one needs to take into account more directly the dislocations local curvature in the matrix channels: perhaps a solution of this problem consists in the use of the generalized continuous media of Cosserat.

At high temperature in particular, these local mechanisms of dislocations lead to strong modifications of the very structure of the precipitates, described in the next section, before presenting simulations which we carried out with our modelling on various standard structures resulting from these evolutions.



Fig. 5: Hydrostatic pressure distribution (in Pa), in the matrix, γ and γ' being viscoplastic.



Fig. 6: ϵ_{33}^p strains distribution in the γ matrix, γ and γ' being viscoplastic.

3. INFLUENCE OF MORPHOLOGICAL MODIFICATIONS

In this section, we evaluate the influence of morphological modifications of the precipitates in the behaviour of the two-phase superalloy. We then carry out calculations on the microstructures in rafts in order to find heterogeneities of plastic strain and stress, related to morphology of these microstructures.

Meissonnier *et al.* show that shape in plate of the precipitates is the most representative structure of the coarsened microstructures /14/. We therefore explore this track:

- on the one hand by a comparison between the simulated curve resulting from a calculation on a rafts mesh

of the type N, and that resulting from another mesh representing the plates,

- on the other hand by comparison between these two curves and the experimental curve.

We thus propose two meshes (type “plates” and raft of the type “N”) which we represent in Figures 7 and 8. These meshes have been carried out from the microscopic observations for the precipitates size, for the distribution of the matrix channels and for the volume fraction (68 % in both cases). In fact, several parameters associated with the precipitate morphology have a great influence: volume fraction, precipitate size in the three directions and relative matrix corridors size. All these parameters condition the construction of the mesh of the coarsened microstructure to study and must be introduced into the used model.

For the calculations which follow, we take again the model shown in Table 1. It takes account of the influence of parameters such as dimensions of the precipitates in the three directions and of the size of the matrix channels and it thus allows modelling correctly the structures in rafts. For reasons of cubic symmetry, and periodicity, the coarsened structure is modelled by an eighth of a parallelepiped with rounded corners included by three half-corridors of the matrix. We authorize the plasticization of the precipitate because we have seen at the time of calculation on a cubic structure that a better simulation is thus obtained /17/.

Several experimental studies have shown that the temperature of 950°C is the seat of notable modifications of the behaviour of the alloy; thus the coefficients of the model are determined and adjusted at this temperature.

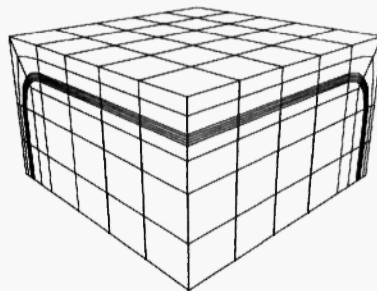


Fig. 7: Mesh of the coarsened microstructure called “plate”.

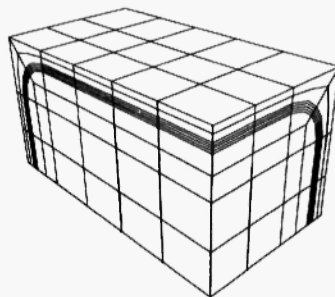


Fig. 8: Mesh of the coarsened microstructure, raft of type N.

4. RESULTS

Calculations are carried out by imposing a uniform displacement, on the higher face of the mesh, up to a strain of 2 %. The boundary conditions imposed are such that the microstructure is periodic and regular.

The calculation results are presented in Figures 9, 10, 11 and 12; the curves obtained represent two

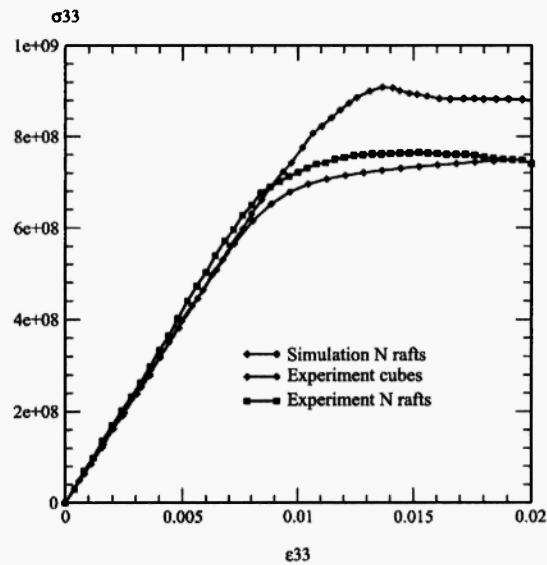


Fig. 9: Comparison between the simulated curves (traction on rafts N), and the experimental ones (cubes and rafts N), for a coarsened microstructure of the AM1 at 950°C (σ_{33} in Pa).

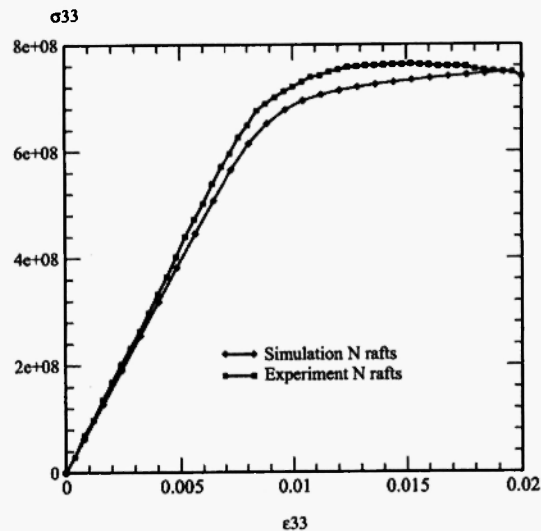


Fig. 10: Comparison between the simulated curves (traction on rafts N), and the experimental one (rafts N), for a coarsened microstructure of the AM1 at 950°C (σ_{33} in Pa).

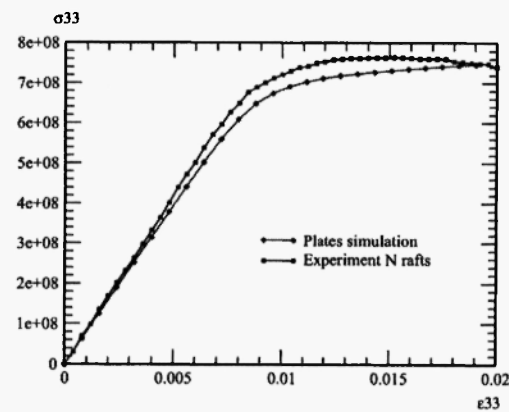


Fig. 11: Comparison between the simulated curves (plate), and the experimental one (rafts N), for a coarsened microstructure of the AM1 at 950°C (σ_{33} in Pa).

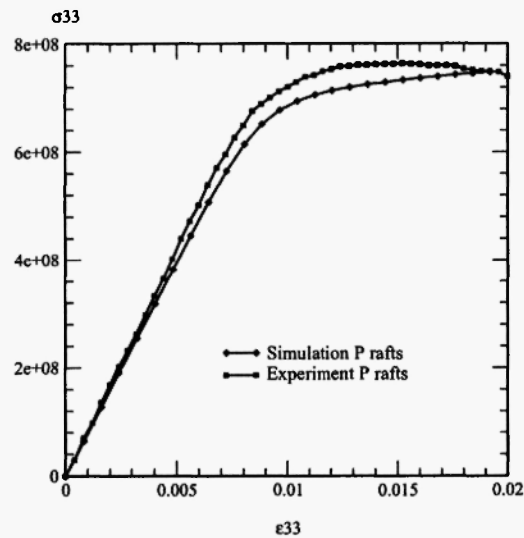


Fig. 12: Comparison between the simulated curves (traction on rafts P), and the experimental one (rafts P), for a coarsened microstructure of the AM1 at 950°C (σ_{33} in Pa).

microstructures N and P. These curves are compared with the experimental curves drawn from the literature in electron microscopy. The experimental tests, from which the traction curves emanate, show a low sensitivity to the precipitates shape. We note, by comparing the simulated curves with those obtained for a cuboid structure, that coarsening is at the origin of a fall of the mechanical characteristics of both structures, which is in conformity with the experimental tests carried out by Espié. It is to be recalled that the change of cubic-rafts morphology modifies appreciably the response of two-phase material, but that the rafts orientation has no significant influence.

The simulated curve resulting from calculation on the mesh of a microstructure in plates is identical to that obtained on a mesh of rafts of the type N. Both non-cuboid structures (rafts of the type N or plates) are equivalent from the modelling point of view. But in agreement with the microscopic observations, the mesh of the microstructure in rafts of the type N is most representative of a coarsened microstructure.

In short, our simulated curves show a good agreement between the finite element calculations and the experimental results; the heterogeneity of the plastic strain, an important character of coarsening, is well represented in the model. In addition, the stress and strain state represented in our Figures 13, 14, 15, 16 and 17, seems to approach the real behaviour of the superalloys in service.



Fig. 13: ϵ_{33}^P strains for rafts of type N of AM1 at 950°C.

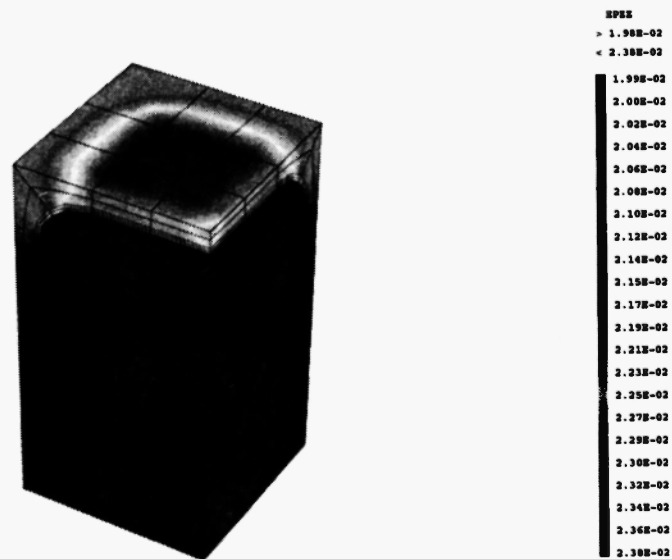


Fig. 14: ϵ_{33}^P strain for rafts of type P of AM1 at 950°C.

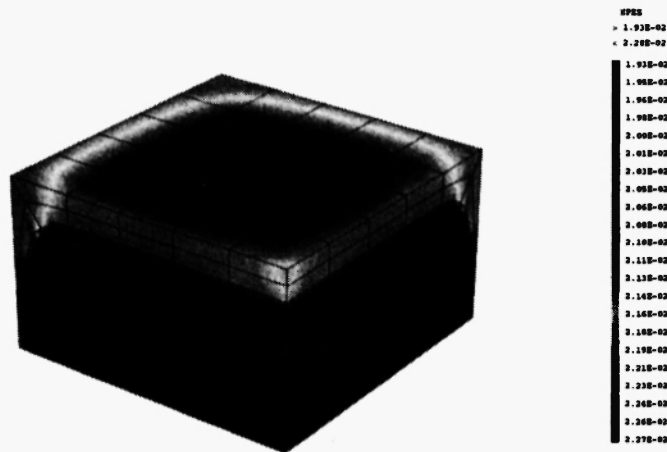


Fig. 15: ε_{33}^P strains for plate structure of AMI à 950°C.



Fig. 16: σ_{33} stresses after traction to 2 % for raft microstructure of type N of AMI at 950°C (σ_{33} in Pa).

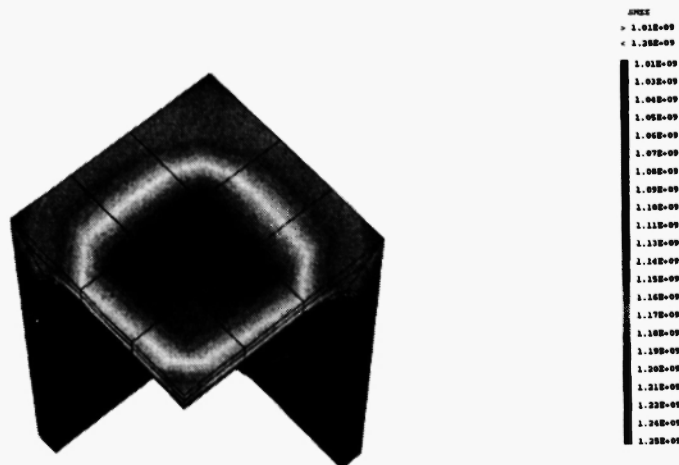


Fig. 17: σ_{33} stresses after traction to 2 % for raft microstructure of type P of AMI at 950°C (σ_{33} in Pa).

5. DISCUSSION

Let us recall initially that, from the elastic energy point of view, the orientation of the rafts P or N is equivalent and that, from this point of view, the structures in rafts are less extensive than the cuboidal structure /12/, which appears to us coherent with what follows in viscoplasticity.

Our calculations show, for rafts of type P, a concentration of strain in the vicinity of the center of a channel perpendicular to the action axis and a strong plastic strain in the channel parallel to the [001] direction, whereas for the rafts of type N, a strong viscoplastic strain is distributed exclusively in the channels perpendicular to the traction axis. Finite elements calculations thus release a strong local sensitivity to the morphological characteristics; as we said previously this fact seems to agree with the few experiments on the subject.

However the experimental tests show a weak global influence of the rafts orientation on the material response, which modelling also confirms; rafts P or N lead to the same behaviour. There are probably differences, however, in the anisotropy of behaviour which should appear for more complex ways of loading, such as non-radial ones.

The reduction in the stress rate, for the modelled coarsened microstructure, towards that obtained on the modelled cuboidal microstructure, characterizes well the effect of coarsening. In view of the results, our coarsened model is in good agreement with the experiment. For the experiment as well as for the model, coarsening thus shows a significant fall in stress compared to the cuboid microstructure.

The behaviour of the coarsened structures is still difficult to explain and describe owing to the fact that the responsible physical mechanisms are associated with the local mechanisms of mobility of dislocations and with important effects of diffusion. However, as the important role of the diffusion in the coarsening contributes to the mitigation of the effect of the discrete behaviour associated with dislocations, one can expect that a phenomenological modelling such as that used here remains more reasonably valid compared with situations of plasticity not accompanied by diffusion. That could explain why our results are in better agreement with the observation for these situations at high temperatures.

6. CONCLUSION

The finite elements methods enabled us to simulate, in a satisfactory way, the mechanical behaviour of the coarsened superalloys, while being based on the microscopic observations of the microstructures; the results of our simulations are in agreement with those proposed in the experimental literature.

It should be noted that the introduction of the effect of the hydrostatic pressure into the matrix behaviour law to model the effect of the morphological modifications in a satisfactory way, would deserve to be better confirmed by more experimental results in electron microscopy.

The model used proves thus to be an effective tool of study of the viscoplasticity of structures of the superalloy type, in a consequent range of temperatures and morphologies. It allows in particular, for various

types of loadings similar to those supported by these materials in service, to evaluate the distributions of stresses in the phases and to obtain indicators of morphological modifications and of other parameters associated.

Finally the model used appears reasonably well adapted for the modelling of the rafts microstructures behaviour. It is all the more remarkable that, to our knowledge, this type of modelling for the rafts had never been carried out until now.

REFERENCES

1. M. Cornet and G. Martin, *Scripta Metallurgica*, **21**, 1091-1095 (1987).
2. A. J. Ardell, *Scripta Metallurgica et Mater.*, **24**, 343-346 (1990).
3. G. Muralidharan and H. Chen, *Science and Technology of Advanced Materials*, **1**, 51-62 (2000).
4. S.G. Tian, H.H. Zhou, J.H. Zhang, H.C. Yang, Y.B. Xu and Z.Q. Hu, *Materials Science and Technology*, **16**, 451-456 (2000).
5. L. Espié, Thèse, juin 1996, ENSMP, Paris.
6. A. Fredholm, "Monocristaux d'alliages base nickel, Relation entre composition, microstructure et comportement en fluage à haute température, Thèse, Ecole des Mines de Paris, 1987.
7. A. Hazotte and A. Simon, *Acta Stereologica*, **8** (2), 175-180 (1989).
8. T. M. Pollock and A. S. Argon, *Acta Metall. Mater.*, **40** (1), 1-30 (1992).
9. P. D. Portella, *Proceedings Mecamat 91*, 1991.
10. M. Ignat, J. Y. Buffiere and J. M. Chaix, *Acta Metall. Mater.*, **41** (3), 855-862 (1993).
11. M. Veron, Thèse, 1995, INP Grenoble.
12. M. Massaoudi, thèse de Doctorat, 2002, UPS-Toulouse.
13. D. Nouailhas and G. Cailletaud, *Scripta Materialia*, **34** (4), 565-571 (1996).
14. F. T. Meisssonier, E. P. Busso and N. P. O'Dowd, *International Journal of Plasticity*, **17**, 601-640 (2001).
15. J. L. Chaboche, S. Lhuillier and D. Nouailhas, IUTAM Symposium on "Transformation Problems in Composite and Active Materials", Y.A. Bahei-El-Din and G.J. Dvorak (Eds.), Kluwer Acad. Publishers, 1998; pp. 33-44.
16. D. Nouailhas and S. Lhuillier, *Computational Materials Science*, **9**, 177-187 (1997).
17. M. Massaoudi, L. Durand and A. Altibelli, "Finite elements modeling of the γ/γ' two-phase viscoplastic behavior", *Journal of the Mechanical Behavior of Materials*, **15** (4-5), 255-277 (2004).

